

Calibration of the Infiltration Rate Curve from the LN Trend Line at Eight Sites of Interest, Based on Infiltration Tests Carried out

Victor Rogelio Tirado Picado 

Faculty of Engineering and Architecture, American University UAM, Managua, Nicaragua

Email: victornica2001@yahoo.com

How to cite this paper: Picado, V.R.T. (2022) Calibration of the Infiltration Rate Curve from the LN Trend Line at Eight Sites of Interest, Based on Infiltration Tests Carried out. *Open Journal of Applied Sciences*, 12, 1098-1115.

<https://doi.org/10.4236/ojapps.2022.127075>

Received: May 27, 2022

Accepted: July 4, 2022

Published: July 7, 2022

Copyright © 2022 by author(s) and Scientific Research Publishing Inc. This work is licensed under the Creative Commons Attribution International License (CC BY 4.0).

<http://creativecommons.org/licenses/by/4.0/>



Open Access

Abstract

The purpose of this research is to demonstrate that a calibration curve can be obtained that can be used for any infiltration test, with the double ring method, as well as an equation that helps speed up data processing. The experimentation was carried out in eight points in Nicaragua, of which five were distributed in Managua and three in Rivas-Nandaime. These results can be used for purposes of other studies of interest. As a result, a calibration curve is obtained, and an expression equal to $y = -87.2 * \ln(x) + 495.64$ is deduced, which will be the equation to determine the average infiltration of a field test occupying the double ring, for a total of 7 hours. And it is from the result that the texture of the soil can be determined by means of the indicator table. The basic methodology allowed analyzing the data since they are obtained, processed and analyzed, resulting in the calibration curve for infiltration tests. Finally, an equation was determined from the averages of the processed data, resulting in a correlation of 0.9976, above 0.5, which means it is very high and reliable.

Keywords

Double Ring, Infiltration, Calibration, Logarithmic Curve, Data Adjustment

1. Introduction

For [1], the infiltration rate curve is obtained from in situ tests of infiltration tests; the recorded data is used for modeling the curve with the LN trend since a curve approaches the following expression: $y = \pm a * \ln(x) \pm b$, where the values “a” and “b” are obtained from statistical analysis.

In theoretical terms, according to [2] infiltration is the process by which the water that reaches the soil surface passes into it. This process is very sensitive to changes in soil management [3]; because, during a test, the instantaneous infiltration rate decreases over time to a constant value called basic infiltration, controlled by the saturated hydraulic conductivity or K_s ; understood as a measure of the flow that crosses a section of the porous system of the saturated soil [4].

Infiltration tests allow knowing the variation of the infiltration capacity as a function of time. The simplest and most widespread tests are those that are developed with concentric rings, in which the data obtained from the field practice are recorded in a spreadsheet measuring the different heights of water and the corresponding times. The time intervals depend on the ground where the measurement is made, and with the height and time data the deltas of both are obtained.

The motivation to carry out this research arises from the need to have basic methodological material for specialists and future professionals, which, adapted to the real conditions of our country, and adapted to the methodologies for hydrogeological infiltration test trials, serve as a theoretical-practical reference in the area, its content implies the review of an extensive bibliography that, in addition to being expensive, is scarce in our country.

2. Objectives

Calibrate the infiltration rate curve using the LN trend line, in order to minimize the steps to obtain an own characteristic curve based on the infiltration tests carried out.

- Define the infiltration rate curve by means of the double ring test.
- To implement a calibration methodology for the infiltration rate curve from eight tests.
- Propose a calibration equation that measures infiltration levels in the soil.

3. Methodological Design

Geographic location of the investigation

In the development of the investigation, to carry out the tests, eight points of interest were obtained, five points in Managua and three points in Nandaime-Rivas, the coordinates of the points are the following: see **Table 1** and **Figure 1**.

Kind of investigation

The present work is designed under the methodological approach of the quantitative approach, since this is the one that best adapts to the characteristics and needs of the investigation.

The quantitative approach uses data collection and analysis to answer research questions and test previously stated hypotheses, and relies on numerical measurement, frequent counting, and the use of statistics to accurately establish patterns of behavior in a series of data [5].

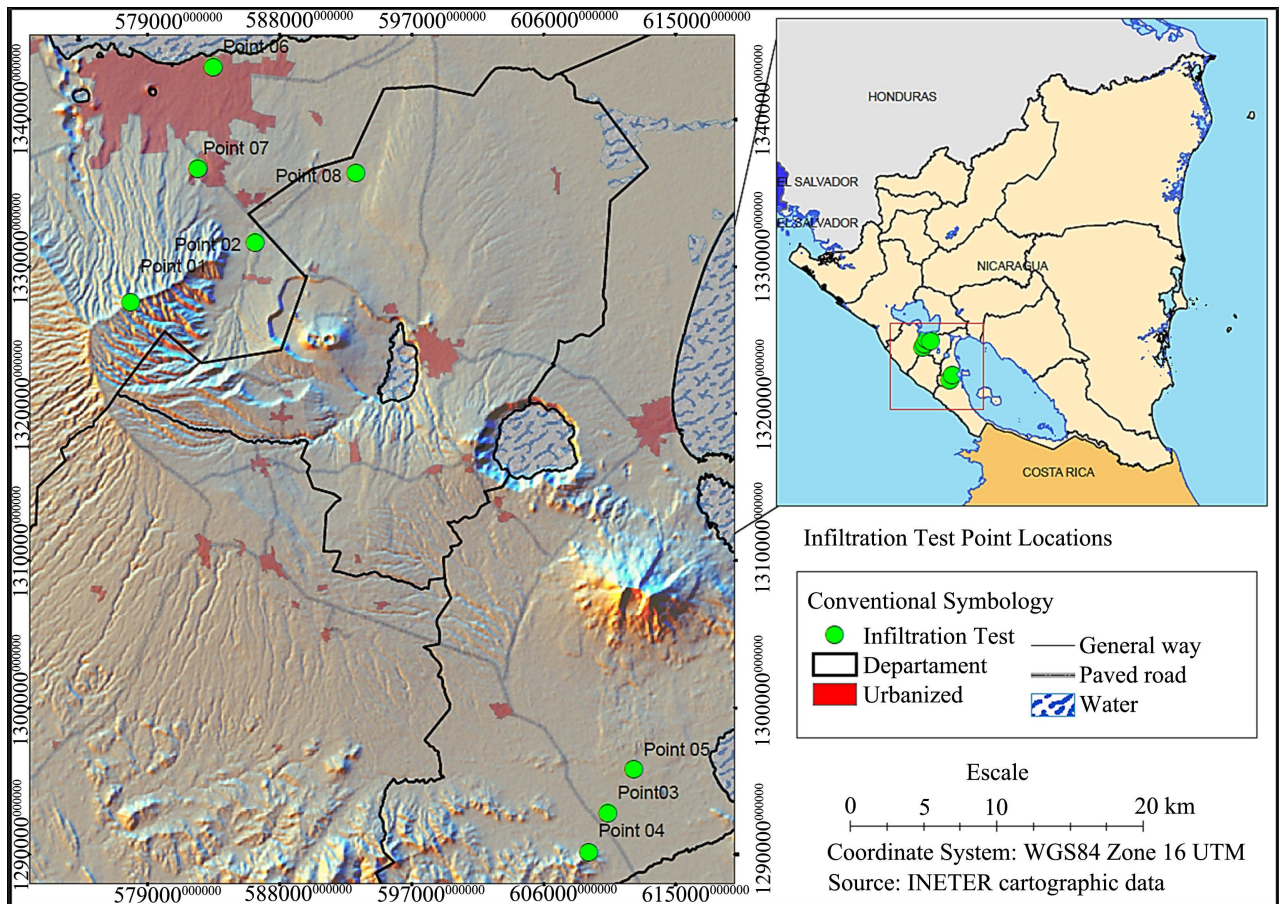


Figure 1. Location of points from coordinates. Source: Self-made (2021). Based on INETER cartographic data.

Table 1. Coordinates of test points.

Point 01	Point 02	Point 03	Point 04	Point 05	Point 06	Point 07	Point 08
1327599.00	1330633.00	1292833.00	1290184.00	1295801.00	1343626.00	1336719.00	1335368.34
577822.00	580157.00	610397.00	609087.00	612151.00	583453.00	582430.00	587037.33

Source: Self-made (2022).

From the quantitative approach, the observation technique will be taken to describe the behavior of the infiltration rate curve by means of the LN trend line, in order to minimize the steps to obtain an own characteristic curve based on the infiltration tests carried out [6].

Execution time

The development of the research to meet the proposed objectives, was carried out in one week, maintaining one trial per day for eight days, the analysis of the data in one week, and one week to present results in the month of October 2021.

Data Collection Techniques and Methods

Primary Sources

On-site observation from infiltration tests carried out at eight different points. Archives of the National Water Authority, (ANA), Nicaragua.

Archives of the Directorate of Water Resources of INETER, Nicaragua

Secondary Sources

Website <https://cenida.una.edu.ni/Tesis/tnp33s211.pdf>

Website <https://geocostarica.com/es/servicios/pruebas-de-infiltracion>

Bibliography related to the topic of infiltration test methods.

Universe

In general, they will be the points determined for the infiltration test in any part of the aquifers of Nicaragua.

Sample

They will be the eight infiltration tests carried out in the aquifers of La Sierras Managua, and Nandaime-Rivas.

Inclusion Criteria

- Only the selected points in the La Sierras Managua and Nandaime-Rivas aquifers.

Exclusion criteria

- All those selected points in other aquifers that are not of interest.

Method

The method consists of saturating a portion of soil limited by two concentric rings, then measuring the variation of the water level in the inner cylinder. This information will help us decide what type of soil is determined [7].

Although it is possible that at the beginning of the experiment, the soil is dry or partially wet and therefore in non-saturated conditions, the initially very high values will drop very quickly as a result of the pressure exerted by the water column, greater it will be the bigger it is [8].

The time that elapses until the final conditions of saturation are reached will depend on the previous humidity, the texture and structure of the soil, the thickness of the horizon through which the water flows, and the height of the water in the inner ring.

The rate or speed of infiltration is the speed with which water penetrates the soil through its surface. We normally express it in mm/h and its maximum value coincides with the hydraulic conductivity of saturated soil [8], see **Figure 2**.

The original method, according to [8], starts from the idea that once the two rings are placed and the saturation situation is obtained (see **Figure 3**), the difference in water level (H) in the inner and outer rings causes a flow of water that will be input to the inner ring (see **Figure 4**) if the height is higher in the outer tube, or output if it is lower (see **Figure 5**).

In any case, in addition to the component of the water flow QH due to the difference in level H between the two rings, the water leaves both cylinders through the surface of the ground in which they are installed as a consequence of its porosity. Therefore, the net flow that leaves (or penetrates in its case) the inner ring is actually the result of two components: the component due to the difference in water level in the rings, the “leakage”; and the component due to the absorption capacity of the soil, infiltration. The problem lies precisely in being able to isolate for each condition of H the component of the “leakage” flow

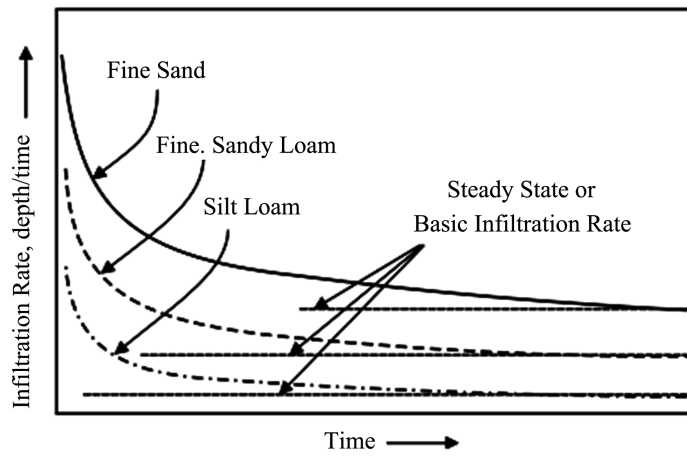


Figure 2. Infiltration rate according to the state of the soil. Source [8].



Figure 3. Double ring infiltrometer Source [9]

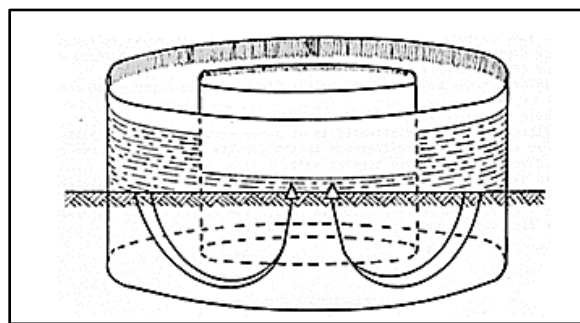


Figure 4. Inlet water flow. Source [9].

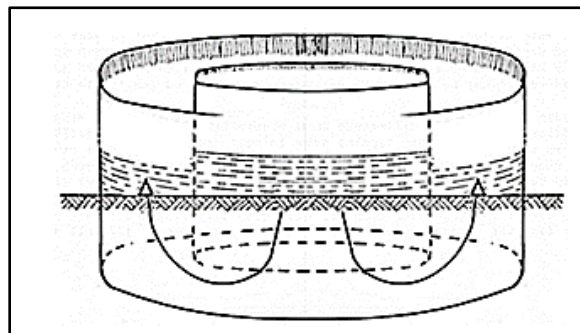


Figure 5. Outlet water flow. Source [9].

from the component of infiltration from the value of the net flow of the inner tube (value object of the measurement). For this, the hypothesis is adopted that the component due to absorption is constant during the performance of the experiment and is not affected by changes in the water level in the inner cylinder, see **Figure 6**.

The hypothesis is indeed valid if the measurements are made in a short space of time and if H remains relatively small. On the other hand, if $H = 0$ then the flow in the inner tube is due solely to soil absorption, this being precisely the purpose of the technique proposed in this section. The outer ring also has the function of preventing the horizontal infiltration of water below the inner cylinder so that the measurements correspond with certainty to the vertical flow.

Materiales y Equipos

- A double ring infiltrometer
- 3 kg mallet
- Strong wood of length that exceeds the outer ring
- A 1 meter tape measure
- 3 buckets or drum
- 1 stopwatch
- 1 GPS
- Table format for gathering field information
- 1 table for support
- 1 graphite pencil

Calculation of Hydraulic Conductivity

To calculate the hydraulic conductivity of the soil in saturated conditions from the measurements obtained during the experience, a table of results will be prepared. It must include as many series as the number of times the inner ring has had to be filled until verifying that the infiltration rate has stabilized. **Table 2** shows an example of a field trial.

[9], reports that the equation that allows determining the accumulated infiltration (I_{acum}) is given by Kotiakov (1932) and improved by Philips (1957) can be indicated by the following expression:

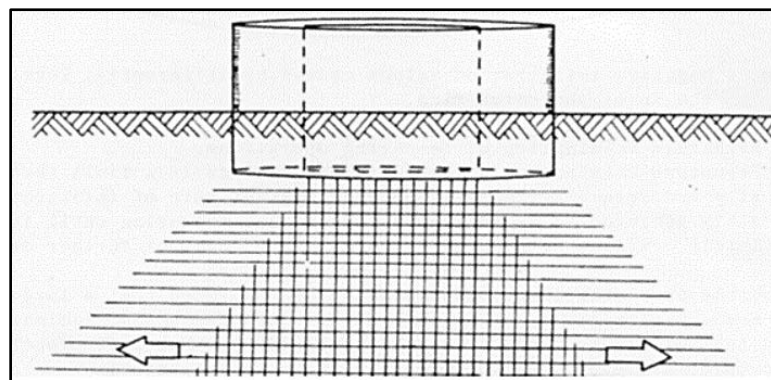


Figure 6. Flow of water in the ground generated by the double ring. Source [9].

Table 2. Field trial example.

Ring n°: Caracteristique of soils	1	Acumulate time	Date: Lecture	Initial time: Cup	Partial foil	Acumulate foil
ID n°	Partial time	minutes	cm	cm	mm	mm
Horas	minutes	minutes	cm	cm	mm	mm
16:00	0	0	0	15	0	0
16:05	5	5	13.5		15	15
16:10	5	10	12.8		7	22
16:15	5	15	12.2	15	6	28
16:20	5	20	14.6		4	32
16:25	5	25	14.2		4	36
16:30	5	30	13.7		5	41
16:40	10	40	12.7	15	10	51
16:50	10	50	14.4		6	57
17:00	10	60	13.6		8	65
17:30	30	90	11.2	15	24	89

Source: [8] and [9].

$$d = K * t^m \tag{1}$$

where:

d = accumulated infiltration at time t (mm);

K = constant that depends on the initial structure of the soil (dry). It is the layer that infiltrates in the first instant greater than zero (mm);

m = constant that depends on the stability of the soil structure against water, $0 > m < 1$;

K in sandy or loamy soils with cracks show values between 10 to 30, soils with stable structures against water show values of m greater than 0.6.

To obtain the values of K and m , the following is done:

$$\log d = \log K + m * \log t \tag{2}$$

equation that responds to the straight line

$$y = b + a * x,$$

where:

$\log d = y$; dependent variable;

$\log K = b$; ordinate at the origin (ground constant);

$m = a$; slope of the line (ground constant);

$\log t = x$; independent variable.

Solving by least squares, we have:

$$m = \frac{\frac{\sum(\log t * \log d)}{n} - \frac{\sum \log t}{n} * \frac{\sum \log d}{n}}{\frac{\sum(\log t)^2}{n} - \left(\frac{\sum \log t}{n}\right)^2} \quad (3)$$

Then Equation (1) is as follows $d = K * t^m$.

To determine the average infiltration rate, we start from the following expression:

$$I = \frac{d}{t} \left(\frac{\text{mm}}{\text{h}} \right) \quad (4)$$

Substituting 1 into 4 we get:

$$I = \frac{d}{t} = \frac{K * t^m}{t} = K * t^{m-1} \quad (5)$$

where:

I = infiltration at a time t (mm/h);

$k = K * m * 60$;

$-n = m - 1$.

Remaining the following expression

$$I = k * t^{-n} \quad (6)$$

The result of the average infiltration is compared with the table related to the soil texture, **Table 3**, the average infiltration is closely related to the soil texture.

4. Results

A summary table of processed data is presented for each point in **Graph 1**. See **Table 4**.

The trend line is presented as a log of the data for each point. See **Graphs 2-5**.

Data adjusted to the logarithmic trend line are presented below, see **Table 5** and **Graph 6**.

From the original data, the average is obtained, it is plotted to obtain a curve that can be adjusted and then define the calibration curve, see **Table 6** and **Graph 7**.

Table 3. Average soil infiltration values (mm/h).

Soil Texture	Basic infiltration. Variation range (mm/h)	Ib average (mm/h)
Sand	25 - 50	50
Sandy Loam	13 - 75	25
Frank	7.5 - 20	12.5
Loamy-loamy	2 - 15	7.5
clay-loam	0.2 - 5	2.6
Clay	0.1 - 1	0.5

Source [9].

Table 4. Data obtained from the tests and processed to obtain I (mm/h).

	Point 01	Point 02	Point 03	Point 04	Point 05	Point 06	Point 07	Point 08
Accumulated Time (min)	Infiltration mm/h	Infiltration mm/h	Infiltration mm/h	Infiltration mm/h	Infiltration mm/h	Infiltration mm/h	Infiltration mm/h	Infiltration mm/h
1	384.119	631.384	332.93	314.71	332.93	338.98	351.78	332.93
2	228.475	625.165	388.71	348.52	393.78	383.68	415.50	393.78
3	216.041	625.685	403.91	389.35	486.69	444.25	512.89	486.69
4	124.662	668.885	437.94	478.04	594.45	531.81	332.93	594.45
5	180.540	308.105	473.76	546.64	321.45	316.00	393.78	235.42
6	133.541	545.552	514.85	323.04	352.06	333.62	506.73	321.45
7	137.625	463.025	336.21	362.11	388.70	353.59	327.09	355.00
8	170.907	516.190	351.89	456.53	401.94	376.45	387.10	374.94
9	177.655	640.131	365.93	496.67	434.52	402.92	495.02	401.94
10	122.457	420.305	411.74	543.03	468.35	457.44	516.10	434.52
12	144.177	364.702	208.69	179.89	257.63	262.08	164.70	234.18
14	189.768	447.221	214.49	221.17	286.43	142.54	191.58	257.63
16	148.815	469.909	232.53	233.80	160.17	178.37	228.47	122.76
18	93.981	594.679	238.84	259.08	172.52	196.59	272.82	160.17
20	120.467	320.700	132.24	285.95	186.89	219.62	162.41	172.52
22	115.410	396.859	162.19	175.76	216.25	249.79	184.47	192.73
24	121.651	412.509	170.21	187.74	222.15	291.38	199.43	204.24
26	128.606	404.742	173.45	209.71	245.05	175.89	240.52	222.15
28	136.405	285.411	179.61	220.46	274.11	207.75	286.61	245.05
30	130.261	337.637	184.35	260.66	323.68	256.45	159.08	274.11
35	141.721	309.394	75.58	113.22	52.51	66.59	71.84	48.01
40	95.281	385.931	77.54	71.12	69.89	78.76	78.64	64.74
45	122.138	290.996	97.56	80.30	76.06	82.04	95.17	69.89
50	123.173	372.206	76.73	92.66	83.61	88.52	104.04	76.06
55	121.894	237.121	82.09	110.37	93.08	96.29	67.80	83.61
60	64.160	234.837	83.92	61.47	105.40	61.13	80.15	93.08
70	112.775	226.703	42.51	43.90	37.29	31.35	51.91	52.36
80	120.062	198.106	42.71	60.16	45.61	33.36	37.29	25.71
90	78.361	197.215	43.26	38.45	58.71	35.36	56.06	37.39
100	91.935	202.028	43.53	54.43	46.53	37.65	36.56	45.48
110	80.814	186.539	44.11	37.07	58.68	38.50	53.62	59.03

Continued

120	89.483	184.087	47.10	38.59	38.55	39.84	35.45	24.95
140	78.197	292.339	16.26	20.70	24.86	21.70	29.72	23.38
160	77.770	168.578	25.59	22.35	18.96	23.55	17.66	28.97
180	71.393	141.940	23.04	22.65	23.00	24.24	27.04	12.97
210	75.705	137.197	17.75	15.58	17.38	10.53	10.90	12.85
240	70.776	138.702	15.45	15.62	12.59	10.03	11.44	16.57
270	70.364	133.243	7.76	7.88	7.04	5.23	6.62	4.44
300	70.776	151.154	7.79	7.98	7.96	5.37	7.72	6.32
360		139.516	7.82	8.10	9.08	5.51	9.34	7.67
420		144.903						

Source: Self-made (2021).

Table 5. Data fitted to the logarithmic trend line for each point.

	Point 01	Point 02	Point 03	Point 04	Point 05	Point 06	Point 07	Point 08
Accumulated Time (min)	Infiltration mm/h	Infiltration mm/h	Infiltration mm/h	Infiltration mm/h	Infiltration mm/h	Infiltration mm/h	Infiltration mm/h	Infiltration mm/h
1	241.57	691.70	496.94	523.73	527.22	500.02	521.87	495.59
2	218.29	622.68	431.53	456.08	458.83	434.60	453.60	430.54
3	204.68	582.31	393.26	416.51	418.82	396.33	413.67	392.49
4	195.02	553.67	366.12	388.43	390.43	369.18	385.33	365.49
5	187.53	531.45	345.06	366.65	368.42	348.12	363.36	344.54
6	181.40	513.29	327.85	348.85	350.43	330.91	345.40	327.43
7	176.23	497.95	313.30	333.81	335.22	316.37	330.22	312.97
8	171.74	484.65	300.70	320.78	322.04	303.76	317.07	300.43
9	167.79	472.92	289.59	309.28	310.42	292.65	305.47	289.38
10	164.25	462.43	279.65	299.00	300.02	282.70	295.09	279.49
12	158.13	444.28	262.44	281.20	282.03	265.49	277.13	262.38
14	152.95	428.93	247.89	266.16	266.82	250.95	261.95	247.91
16	148.47	415.63	235.29	253.13	253.65	238.34	248.80	235.38
18	144.51	403.91	224.18	241.63	242.03	227.23	237.20	224.33
20	140.97	393.41	214.23	231.35	231.63	217.28	226.82	214.44
22	137.77	383.92	205.24	222.04	222.23	208.29	217.43	205.50
24	134.85	375.26	197.03	213.55	213.64	200.08	208.86	197.33
26	132.16	367.29	189.47	205.74	205.74	192.52	200.98	189.82
28	129.67	359.91	182.48	198.51	198.43	185.53	193.68	182.86

Continued

30	127.36	353.04	175.97	191.77	191.62	179.01	186.89	176.39
35	122.18	337.69	161.42	176.73	176.41	164.47	171.70	161.92
40	117.70	324.40	148.82	163.70	163.24	151.86	158.55	149.39
45	113.74	312.67	137.71	152.20	151.62	140.75	146.95	138.33
50	110.20	302.18	127.76	141.92	141.22	130.80	136.57	128.45
55	107.00	292.69	118.77	132.61	131.82	121.81	127.19	119.50
60	104.08	284.03	110.56	124.12	123.23	113.60	118.62	111.34
70	98.91	268.68	96.01	109.08	108.02	99.05	103.44	96.87
80	94.42	255.38	83.41	96.04	94.85	86.44	90.28	84.34
90	90.47	243.65	72.29	84.55	83.22	75.33	78.68	73.28
100	86.93	233.16	62.35	74.27	72.83	65.38	68.31	63.39
110	83.73	223.67	53.36	64.96	63.42	56.39	58.92	54.45
120	80.81	215.01	45.14	56.47	54.84	48.18	50.35	46.28
140	75.63	199.66	30.60	41.43	39.63	33.63	35.17	31.82
160	71.15	186.36	18.00	28.39	26.45	21.03	22.02	19.28
180	67.19	174.64	6.88	16.90	14.83	9.91	10.42	8.23
210	62.01	159.29		1.85				
240	57.53	145.99						
270	53.57	134.27						
300	50.04	123.77						
360	43.91	105.62						
420	38.74	90.27						

Source: Self-made (2021).

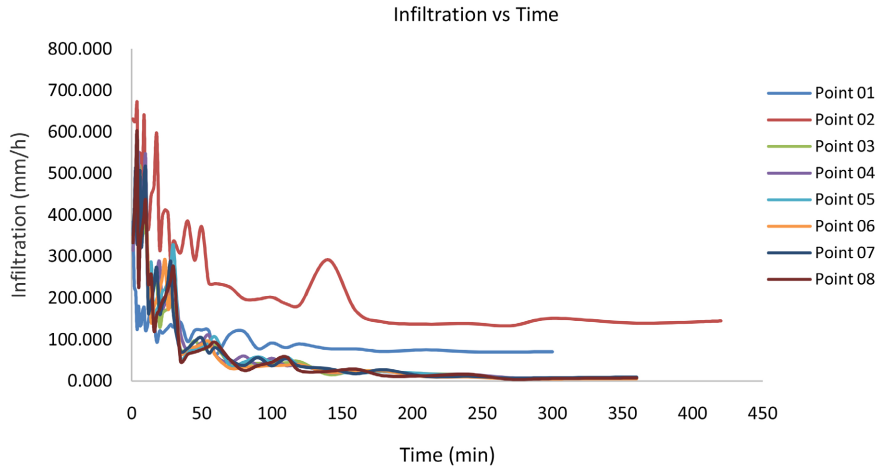
Table 6. The calculation of the average with which one works to determine the calibration of the curve is shown.

	Point 01	Point 02	Point 03	Point 04	Point 05	Point 06	Point 07	Point 08	Average
Accumulated Infiltration Time (min)	Infiltration mm/h	Infiltration mm/h	Infiltration mm/h	Infiltration mm/h	Infiltration mm/h	Infiltration mm/h	Infiltration mm/h	Infiltration mm/h	Infiltration mm/h
1	384.119	631.384	332.93	314.71	332.93	338.98	351.78	332.93	377.471
2	228.475	625.165	388.71	348.52	393.78	383.68	415.50	393.78	397.202
3	216.041	625.685	403.91	389.35	486.69	444.25	512.89	486.69	445.688
4	124.662	668.885	437.94	478.04	594.45	531.81	332.93	594.45	470.395
5	180.540	308.105	473.76	546.64	321.45	316.00	393.78	235.42	346.963
6	133.541	545.552	514.85	323.04	352.06	333.62	506.73	321.45	378.856
7	137.625	463.025	336.21	362.11	388.70	353.59	327.09	355.00	340.420

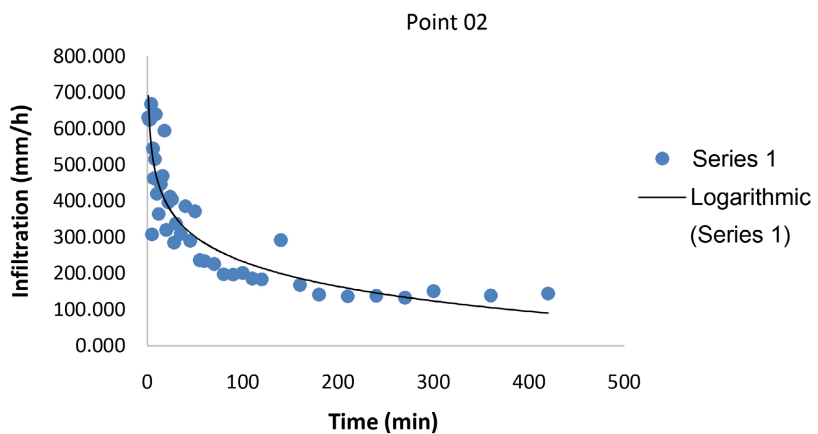
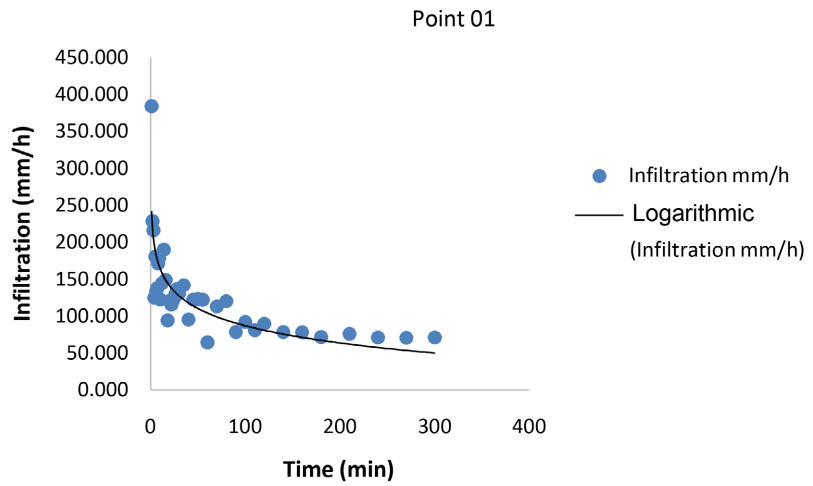
Continued

8	170.907	516.190	351.89	456.53	401.94	376.45	387.10	374.94	379.493
9	177.655	640.131	365.93	496.67	434.52	402.92	495.02	401.94	426.847
10	122.457	420.305	411.74	543.03	468.35	457.44	516.10	434.52	421.743
12	144.177	364.702	208.69	179.89	257.63	262.08	164.70	234.18	227.007
14	189.768	447.221	214.49	221.17	286.43	142.54	191.58	257.63	243.854
16	148.815	469.909	232.53	233.80	160.17	178.37	228.47	122.76	221.853
18	93.981	594.679	238.84	259.08	172.52	196.59	272.82	160.17	248.586
20	120.467	320.700	132.24	285.95	186.89	219.62	162.41	172.52	200.098
22	115.410	396.859	162.19	175.76	216.25	249.79	184.47	192.73	211.680
24	121.651	412.509	170.21	187.74	222.15	291.38	199.43	204.24	226.163
26	128.606	404.742	173.45	209.71	245.05	175.89	240.52	222.15	225.014
28	136.405	285.411	179.61	220.46	274.11	207.75	286.61	245.05	229.425
30	130.261	337.637	184.35	260.66	323.68	256.45	159.08	274.11	240.777
35	141.721	309.394	75.58	113.22	52.51	66.59	71.84	48.01	109.855
40	95.281	385.931	77.54	71.12	69.89	78.76	78.64	64.74	115.236
45	122.138	290.996	97.56	80.30	76.06	82.04	95.17	69.89	114.269
50	123.173	372.206	76.73	92.66	83.61	88.52	104.04	76.06	127.125
55	121.894	237.121	82.09	110.37	93.08	96.29	67.80	83.61	111.531
60	64.160	234.837	83.92	61.47	105.40	61.13	80.15	93.08	98.018
70	112.775	226.703	42.51	43.90	37.29	31.35	51.91	52.36	74.849
80	120.062	198.106	42.71	60.16	45.61	33.36	37.29	25.71	70.375
90	78.361	197.215	43.26	38.45	58.71	35.36	56.06	37.39	68.101
100	91.935	202.028	43.53	54.43	46.53	37.65	36.56	45.48	69.767
110	80.814	186.539	44.11	37.07	58.68	38.50	53.62	59.03	69.795
120	89.483	184.087	47.10	38.59	38.55	39.84	35.45	24.95	62.254
140	78.197	292.339	16.26	20.70	24.86	21.70	29.72	23.38	63.394
160	77.770	168.578	25.59	22.35	18.96	23.55	17.66	28.97	47.928
180	71.393	141.940	23.04	22.65	23.00	24.24	27.04	12.97	43.284
210	75.705	137.197	17.75	15.58	17.38	10.53	10.90	12.85	37.237
240	70.776	138.702	15.45	15.62	12.59	10.03	11.44	16.57	36.398
270	70.364	133.243	7.76	7.88	7.04	5.23	6.62	4.44	30.322
300	70.776	151.154	7.79	7.98	7.96	5.37	7.72	6.32	33.132
360		139.516	7.82	8.10	9.08	5.51	9.34	7.67	26.719
420		144.903							

Source: Self-made (2021).

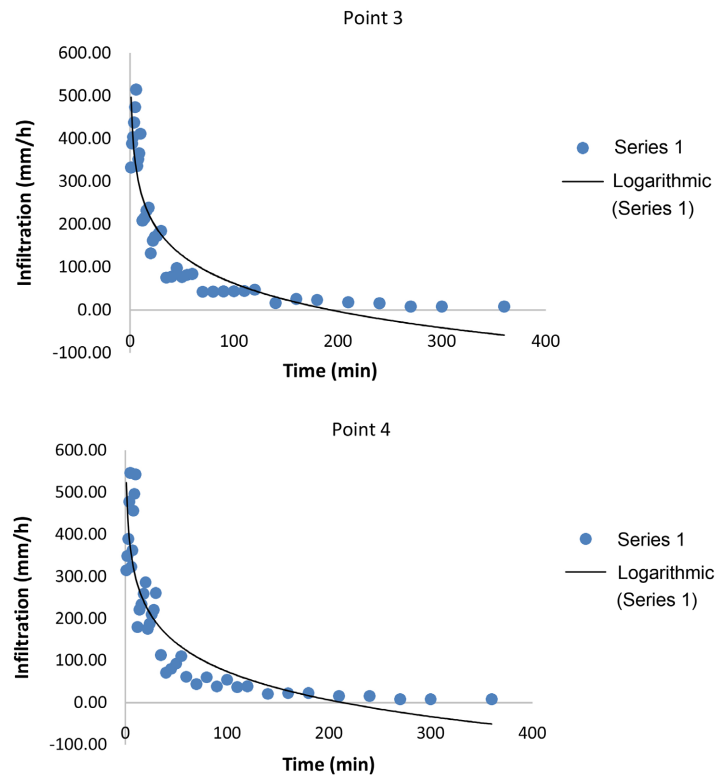


Graph 1. The behavior of the infiltration is shown for each of the points. Source: Self-made (2021).

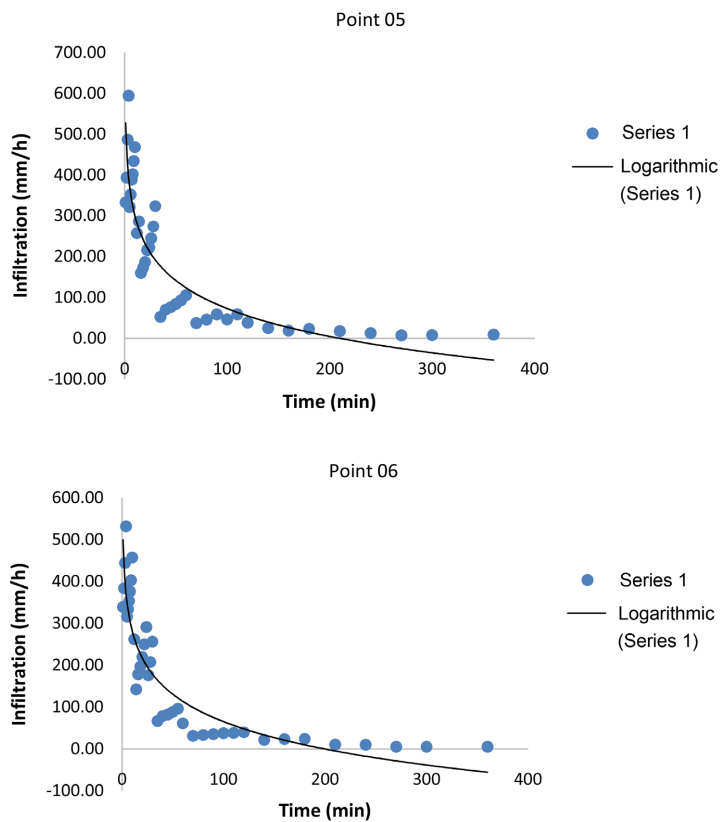


Graph 2. Trend line with data from point 1 and 2. Source: Self-made (2021).

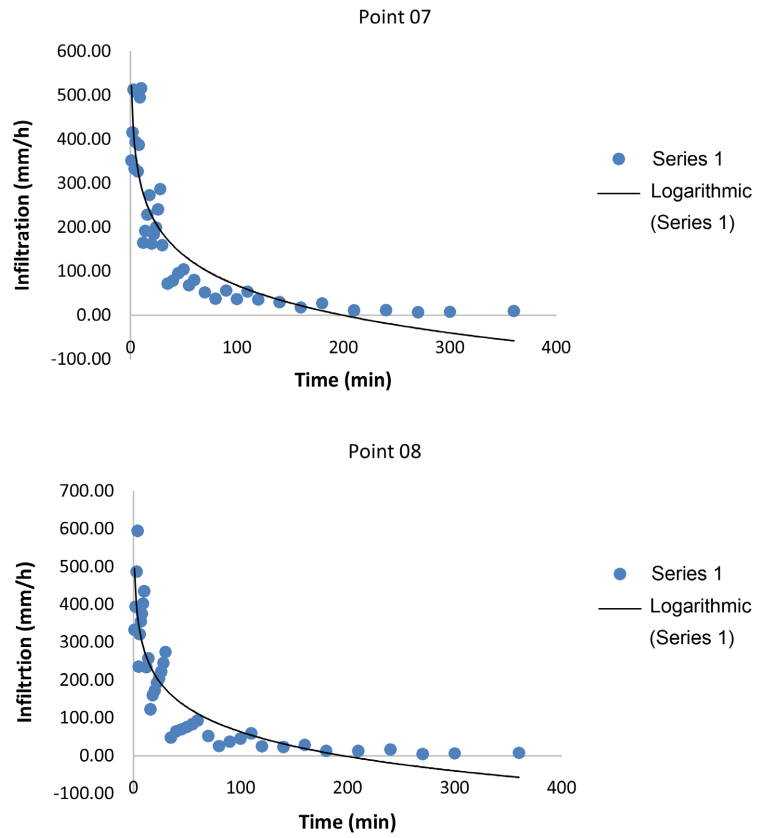
Next, the calibration of the curve is presented to determine the infiltration in a period of 7 hours, see **Table 7** and **Table 8**, **Graph 8**.



Graph 3. Trend line with data from point 3 and 4. Source: Self-made (2021).



Graph 4. Trend line with data from point 5 and 6. Source: Self-made (2021).

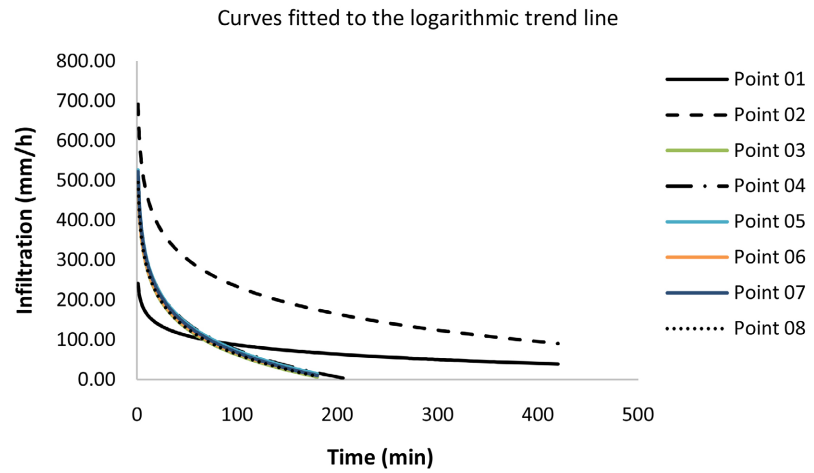


Graph 5. Trend line with data from point 7 and 8. Source: Self-made (2021).

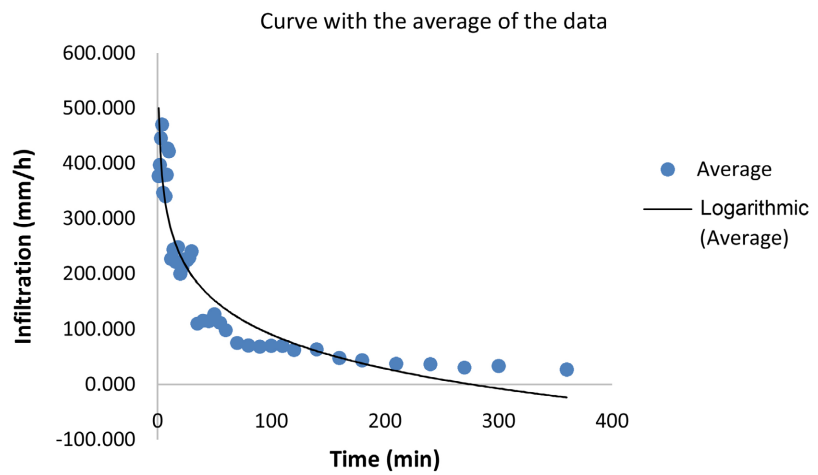
Table 7. Dates for the graphic.

Accumulated Time (min)	Infiltration mm/h	Accumulated Time (min)	Infiltration mm/h	Accumulated Time (min)	Infiltration mm/h
1	500.53	20	233.67	90	99.69
2	438.78	22	225.18	100	90.30
3	402.67	24	217.43	110	81.81
4	377.04	26	210.30	120	74.06
5	357.16	28	203.70	140	60.33
6	340.92	30	197.55	160	48.43
7	327.19	35	183.82	180	37.94
8	315.29	40	171.92	210	24.21
9	304.80	45	161.43	240	12.31
10	295.42	50	152.05	270	1.82
12	279.17	55	143.56	300	0.90
14	265.44	60	135.81	360	0.60
16	253.55	70	122.07	420	0.50
18	243.06	80	110.18		

Source: Self-made (2021).



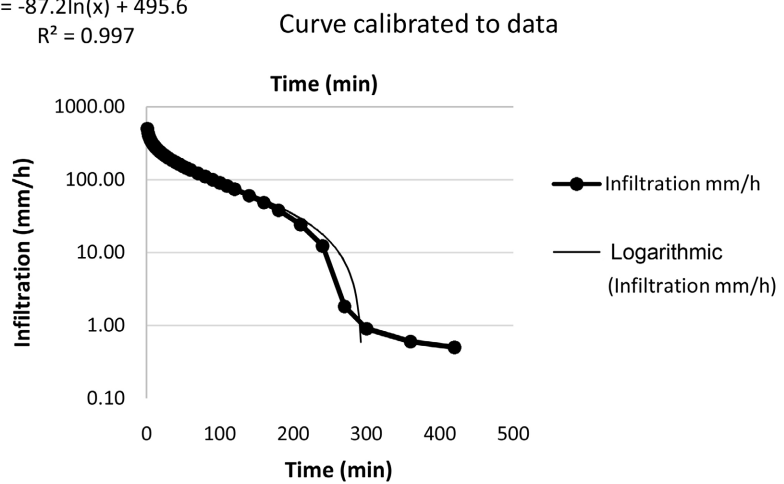
Graph 6. Curves fitted to the logarithmic trend line for each point are shown. Source: Self-made (2021).



Graph 7. The curve with the average of the data is shown. Source: Self-made (2021).

$$y = -87.2\ln(x) + 495.6$$

$$R^2 = 0.997$$



Graph 8. The curve calibrated to the data with a correlation of 0.9976 is shown. Source: Self-made (2021).

Table 8. Basic infiltration variation range.

Soil Texture	Basic infiltration. Variation range (mm/h)	Ib average (mm/h)
Sand	25 - 50	50
Sandy Loam	13 - 75	25
Frank	7.5 - 20	12.5
Loamy-loamy	2 - 15	7.5
clay-loam	0.2 - 5	2.6
Clay	0.1 - 1	0.5

Source [9].

5. Analysis of the Results

From the calibration curve, an expression equal to

$$y = -87.2 * \ln(x) + 495.64,$$

which will be the equation to determine the average infiltration of a field test occupying the double ring, for a total of 7 hours. And it is from the result that the texture of the soil can be determined by means of the indicator table.

6. Conclusions

The infiltration rate curve was successfully defined by applying the double ring theory, following a basic methodology.

The basic methodology allowed analyzing the data since they are obtained, processed and analyzed, resulting in the calibration curve for infiltration tests.

Finally, an equation was determined from the averages of the processed data, resulting in a correlation of 0.9976, above 0.5, which means it is very high and reliable.

Acknowledgements

First of all, to God, our father, who has given me a hand to continue on the right path as a person.

To my mother Beatriz Picado, for teaching me the path to success.

To my children Dafned Itziar Tirado Flores, and Víctor Manuel Tirado Flores, I will always be your guide.

To my wife, Lisseth Carolina Blandon Chavarría, who trusts in my successes, thank you for being by my side.

To the American University (UAM) and Faculty of Engineering and Architecture (FIA), for opening the doors of knowledge to me in this new stage of my life.

Financing

Own budget, and contribution from the American University.

As for technical support, there was the participation of two specialists in the area of hydrogeology.

Conflicts of Interest

The author declares no conflicts of interest regarding the publication of this paper.

References

- [1] Geo Costa Rica (2021).
<https://geocostarica.com/es/servicios/pruebas-de-infiltracion>
<https://geocostarica.com>
- [2] Aranda, D.F.C. (1992) Procesos Del Ciclo Hidrológico, Universidad Autónoma de San Luis Potosí, San Luis Potosí, México.
- [3] Davidoff, B. and Selim, H.M. (1986) Goodness of Fit for Eight Water Infiltration Models. *Soil Science Society of America Journal*, **50**, 759-764.
<https://doi.org/10.2136/sssaj1986.03615995005000030039x>
- [4] Amoozegar, A. (1992) Compact Constant Head Permeameter: A Convenient Device for Measuring Hydraulic Conductivity. In: Topp, G.C., Reynolds, W.D. and Green, R.E., Eds., *Advances in Measurement of Soil Physical Properties: Bringing Theory into Practice*, Soil Science Society of America, Madison, 31-42.
<https://doi.org/10.2136/sssaspecpub30.c3>
- [5] Hernández Sampieri, R. and Fernández Collado, C. (2014) Metodología de la Investigación. McGraw-Hill Interamericana Editores, S.A. DE C.V, Ciudad de México.
- [6] Chow, V., Maidment, D.R. and Mays, L.W. (1994) Hidrología Aplicada. McGraw-Hill Interamericana, Santa Fe, Colombia.
- [7] Sáenz, G.M. (1999) Hidrología en la Ingeniería. Marcombo, Barcelona.
- [8] Génova, L., Andreau, R., Etcheverry, M., Etchevers, P., Chale, W., Calvo, L. and Ramos, F. (2021).
https://aulavirtual.agro.unlp.edu.ar/pluginfile.php/15618/mod_resource/content/2/unidad%20%202017.pdf
<https://aulavirtual.agro.unlp.edu.ar>
- [9] PROSAP (2021).
http://www.prosap.gov.ar/Docs/INSTRUCTIVO%20_R014_%20infiltrometro%20doble%20anillo.pdf
<http://www.prosap.gov.ar/>